Simulation Based on COMSOL for Effect of Electrode Configuration on 1D-BPM

Gao Wenhong Ma Shuyuan

(*School of Mechanical and Vehicular Engineering, Beijing Institute of Technology, Beijing* 100081, *China*)

Abstract One-dimensional dimension binary-code phase modulator (1D-BPM) for speckle reduction in laser display system is designed based on $Pb(Mg_{1/3}Nb_{2/3})O_3$-$PbTiO_3$ (PMN-PT) and microelectromechnical system (MEMS) microfabrication technology. Mathematical model of 1D-BPM is built up, and the relationship between phase shift and electrical field applied by electrodes is deduced. Electrode configuration is investigated by simulation with finite element analysis. We find that the phase distribution across the gap between two electrodes depends not only on the electric field applied by electrodes, but also on the electrodes′ configuration when their dimensions are on the submicron order. Electrodes corner effect is the significant factors for device design and optimization.

Key words laser technique; PMN-PT; speckle reduction; finite element analysis; speckle

中图分类号 TN24 **文献标识码** A **doi**: 10.3788/LOP49.081401

利用 COMSOL 软件对 1D-BPM 电极影响的仿真及分析

高文宏 马树元

(北京理工大学机械与车辆工程学院, 北京 100081)

摘要 基于微机电系统(MEMS)微加工技术和 $Pb(Mg_{1/3}Nb_{2/3})O_3$-$PbTiO_3$(PMN-PT)电光材料设计的一维二进制码相位调制器(1D-BPM)可用于激光显示技术中的散斑消除。建立了 1D-BPM 数学模型,推导出电极在 PMN-PT 片内产生的电场和 PMN-PT 折射率变化导致通过的光束相位变化的关系。采用有限元分析方法仿真了电极几何尺寸对相位的影响,发现当电极尺寸在亚微米级时,两电极间相位分布不仅依赖于电极产生的电场大小,而且受到电极几何尺寸的影响。电极角效应是器件设计及优化时需考虑的重要因素。

关键词 激光技术; PMN-PT; 散斑消除; 有限元分析; 散斑

OCIS codes 140.0140; 030.0030

1 Introduction

Lasers have been thought perfect light source to replace the conventional lamps in projection displays because they have many advantages such as broader color gamut for natural vivid color image, energy efficient electrical-to-optical conversion, longer lifetime and small etendue hence high contrast and reduced size of the projector optics. However, when the coherent laser beam is scattered from optically rough surface such as screen, the speckle noise pattern is received by a square-law detector with a finite aperture[1] such as human eye. Speckle noise patterns typically appear as random bright and dark areas, masking the useful information during the display. Many methods of speckle reduction have been developed in the past fourty years. At present, these methods can be classified into three categories, 1) laser spatial coherence reduction, 2) laser temporal coherence reduction, and 3) spatial or temporal averaging of the speckle images.

收稿日期: 2012-01-08; **收到修改稿日期**: 2012-02-15; **网络出版日期**: 2012-05-22

作者简介: 高文宏(1977—),男,博士研究生,主要从事激光显示技术中散斑消除方面的研究。

E-mail: wenhong.gaw@gmail.com

导师简介: 马树元(1960—),男,教授,博士生导师,主要从事检测控制技术和机电一体等方面的研究。

E-mail: bitmc@bit.edu.cn

Trisnadi *et al*.[2~4] have done investigations on speckle reduction by using movable diffusers based on two-dimensional (2D) Hadamard binary phase matrices in projection displays. A movable Hadamard binary phase matrix, also called phase diffuser, is employed at the intermediate image plane for speckle reduction. Under each pixel of the picture, a 2D time varying binary phase pattern is exposed sequentially which helps bring the speckle reduction by averaging the time-varying speckle pattern at each picture pixel due to finite integration time of the detector such as human eye-brain system.

A sub-matrix formed by any row of Hadamard matrix of order $M = N_1 \times N_2$ generated by the Sylvester construction is equivalent to the outer product of the row vector $\boldsymbol{A}(i)$ of length N_2 and the corresponding column vector $\boldsymbol{B}(i)$ of length N_1[5]. According to this characteristic, a newer approach is proposed for laser speckle reduction in laser projection display. M pairs of vectors $\boldsymbol{A}(i)$ and $\boldsymbol{B}(i)$, also called one-dimensional binary-code phase modulators (1D-BPMs) are generated to replace Trisnadi's diffuser at an intermediate image plane to reduce the laser speckle. By configuring a pair of 1D-BPMs in orthogonal orientation, light phase modulation via the pair of time-varying 1D-BPMs is equivalent to that of the time-varying 2D-BPMs[5].

To have the concept verified by experiments, a pair of 1D-BPMs and their corresponding 2D-BPM with Hadamard matrix of order $H(64)$ are designed. Using $H(64)$ matrix means that under each picture pixel, patterned photoresist on glass wafer is vibrating on the image plane under 632 nm wavelength. The experimental result agrees well with the theoretical value of speckle contrast 8.84% $(1/\sqrt{2}\times 1/\sqrt{64})$.

By using the dynamic 1D-BPMs instead of 2D-BPM, the number of control electrodes is significantly reduced, and the control electrodes change from a 2D distribution to a 1D distribution, which enables a simpler processing technology for fabricating the phase diffuser. To avoid vibratory motion of phase diffusers, electro-optical (EO) implementation can be employed to generate a dynamic phase modulator actuated electrically.

EO material is a good choice for 1D-BPMs because the refraction index hence the phase pattern behind 1D-BPMs can be changed by applying the electric field. The high electro-optical coefficient is the key component of an EO-type material. Shames *et al*.[6~8] developed the spatial light modulator (SLM) by lanthanum-modified lead zirconate titanate (PLZT) 9.0/65/35 material and interdigital surface electrodes (ISEs). Song[9,10] proposed her SLM with PLZT and indium tin oxide (ITO) electrodes. However, its significant field-induced and polarization-dependent scattering losses and high hysteresis made it problematic in controlling dynamic devices. The newly developed modified $Pb(Mg_{1/3}Nb_{2/3})O_3$-$PbTiO_3$ (PMN-PT) ceramic has greatly alleviated the aforementioned issues.

2 Theory

Fig. 1 shows the phase modulation of light by 1D-BPMs and 2D-BPM. Fig. 2 shows the measured speckle patterns. It is seen that similar results can be obtained with these configurations.

Thin wafers of PMN-PT are isotropic at room temperature due to its cubic crystallographic structure, whose index ellipsoid follows[11]

$$(x^2 + y^2 + z^2)/n^2 = 1, \tag{1}$$

where n is the refractive index.

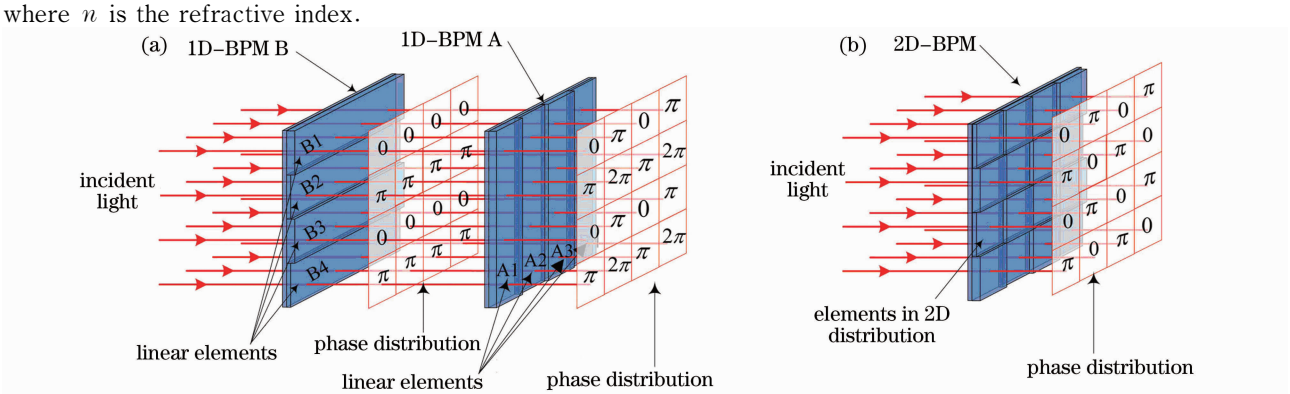

Fig. 1 Schematic presentation for phase modulation of light by (a) 1D-BPM plate pair and (b) a single 2D-BPM

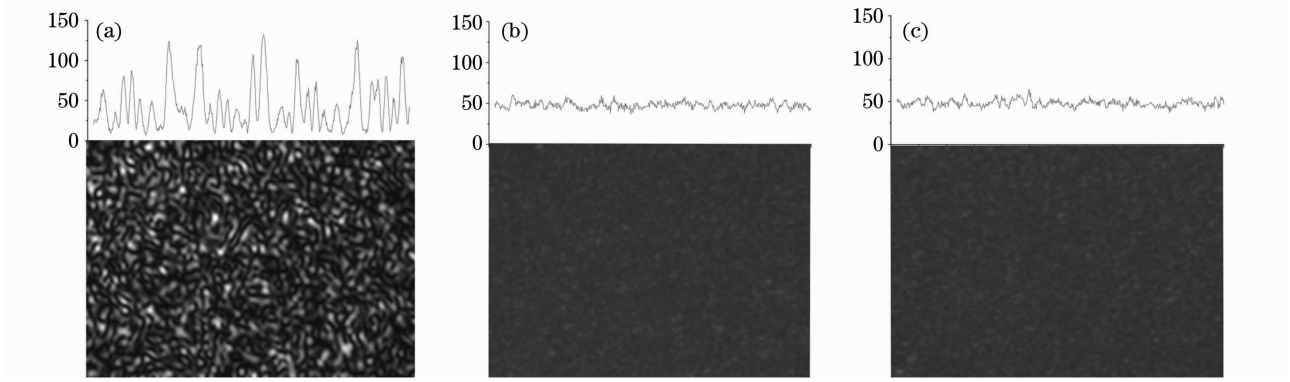

Fig. 2 Measured speckle patterns. (a) Without phase diffuser, speckle contrast is 70%; (b) with a single 2D-BPM, speckle contrast is 8.8%; (c) with the set of 1D-BPM; speckle contrast is 8.96%[5]

When an external electric field E is applied, the PMN-PT will be polarized. The electric field is constructed by components E_x, E_y, E_z:

$$E^2 = E_x^2 + E_y^2 + E_z^2. \tag{2}$$

The 1D-BPMs are constructed by stripe-shaped metal electrodes of width d and length L on the surface of PMN-PT wafer. A light beam passes through the 1D-BPMs within the gap between two electrodes. An applied electric field E across such electrodes creates curved lines of electric field within the wafer, as shown in Fig. 3. Assuming the electrode length $L \gg d$, therefore $E_z = 0$, it means there is no electric field effect in the z direction.

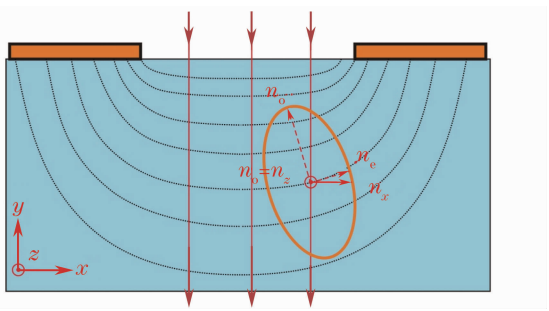

Fig. 3 Electric field distribution in 1D-BPM

PMN-PT polarized by electric field is usually modeled as a uniaxial crystal with the principal index ellipsoid given by[11]

$$(x^2 + y^2)/n_o^2 + z^2/n_e^2 = 1, \tag{3}$$

where n_o and n_e are the refractive indices in ordinary direction and extraordinary direction, which are functions of electrical field E, EO coefficient and refractive index:

$$n_o = n + \frac{1}{2}n^3 R_{12} E^2, \qquad n_e = n + \frac{1}{2}n^3 R_{11} E^2, \tag{4}$$

where R_{11}, R_{12} are the EO coefficients in 11 and 12 directions in R_{mn} matrix.

Since the direction of optical axis changes according to the direction of the applied electric field, the index ellipsoid's optical axis orientation will vary as a function of position within the EO wafer. The refraction indices parallel and perpendicular to the surface electrodes n_z and n_x can be approximated[12] as

$$n_z = n_o, \qquad n_x = \left\{\frac{\cos^2[\theta(x,y)]}{n_e^2} + \frac{\sin^2[\theta(x,y)]}{n_o^2}\right\}^{-1/2}, \tag{5}$$

where $\theta(x,y) = \arctan\left[\dfrac{E_y(x,y)}{E_x(x,y)}\right]$.

The differences of refraction index with and without electrical field in z and x directions are

$$\Delta n_z = n_z - n = \frac{1}{2}n^3 R_{12} E^2, \qquad \Delta n_x = n_x - n = \left\{\frac{\cos^2[\theta(x,y)]}{n_e^2} + \frac{\sin^2[\theta(x,y)]}{n_o^2}\right\}^{-1/2} - n. \tag{6}$$

Using Taylor series expansion, Eq. (6) can be approximated by

$$\Delta n_x = n_x - n = n_o - (n_o - n_e) \times \cos^2[\theta(x,y)] - n = \frac{n^3 E^2(x,y)}{2}\{R_{12} - (R_{12} - R_{11})\cos^2[\theta(x,y)]\}.$$

Since $\theta(x,y) = \arctan\left[\dfrac{E_y(x,y)}{E_x(x,y)}\right]$, then

$$\Delta n_x = \frac{n^3}{2}[R_{12}E_y^2(x,y) + R_{11}E_x^2(x,y)]. \tag{7}$$

Therefore, the phase shifts of the parallel (z direction) and perpendicular (x direction) polarization components are determined, when light beam passing through the 1D-BPMs, by

$$\begin{cases} \Phi_x(x) = \dfrac{2\pi}{\lambda}\int_{y=0}^{l}\Delta n_x \mathrm{d}y = \dfrac{\pi n^3}{\lambda}\int_{y=0}^{l}[R_{12}E_y^2(x,y)+R_{11}E_x^2(x,y)]\mathrm{d}y \\ \Phi_z(x) = \dfrac{2\pi}{\lambda}\int_{y=0}^{l}\Delta n_z \mathrm{d}y = \dfrac{\pi n^3}{\lambda}\int_{y=0}^{l}R_{12}E^2(x,y)\mathrm{d}y \end{cases}, \tag{8}$$

where λ is the wavelength in vacuum and l is the thickness of PMN-PT wafer.

Under 12 μm × 12 μm one-pixel area, $M^{1/2}$ = 4 electrodes on one 1D-BMP of Hadamard matrix of order M = 16 are employed to change the phase pattern of light beam. The distance is 3 μm between two electrodes, and the electrodes should be narrower for less light lost. A uniform phase distribution like 0 or π across the gap between two electrodes is required for reducing speckle well. COMSOL commercial program provideing finite element analysis (FEA) tool can calculate the electric field induced by metal electrodes and the phase distribution across the gap between two electrodes.

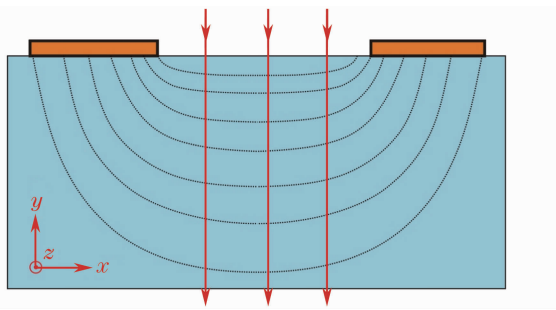

Fig. 4 1D-BPM simulation model

3 Simulation

A model is built up in COMSOL software according to the structures of 1D-BPMs. The electrodes are arranged with equal distance of 3 μm on the PMN-PT wafer surrounded by air, as shown in Fig. 4. The electric field distribution in PMN-PT is determined by electrodes. In this model, the phase distribution across the gap between two electrodes is simulated.

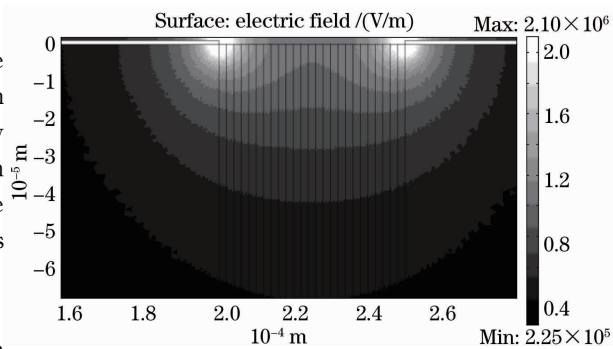

Fig. 5 Electrical field distribution inside the PMN-0.08PT wafer

PMN-0.08PT′s EO coefficients are about $R_{11}=1.4\times10^{-16}$ m²/V² and $R_{12}=0.09\times10^{-16}$ m²/V² for 532 nm wavelength at room temperature. The refraction index n is 2.65 without electrical field effect[13]. The thickness of PMN-0.08PT wafer l is about 1.5 mm. When a voltage is applied on adjacent electrodes, the electrical field will be generated inside the PMN-PT material, as shown in Fig. 5. By integrating the phase change along y direction following Eq. (8), the phase shifts of parallel (z direction) and perpendicular (x direction) polarization components will be got according to the electrical field distribution in PMN-0.08PT wafer.

To uniform the phase distribution, the influence of electrode width is investigated. The retarded phase versus the gap between two electrodes in x and z directions is shown in Fig. 6.

The simulation result shows that phase distribution is going to be uniform when the width of electrodes is reduced from 1 μm to 0.3 μm. The retarded phase is from π to 1.43π. However, when the width of electrodes is

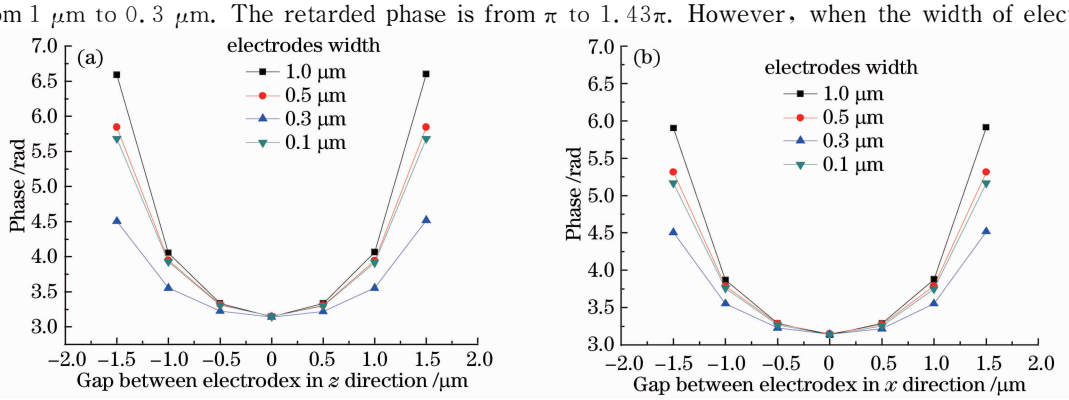

Fig. 6 Phase distributions with difference electrode widths

further reduced to 0.1 μm, the phase distribution will be curved due to the electrodes corner effect. The narrower is the electrode, the nearer are the two corners on bottom of electrodes. This effect will lead to high electrical field inside the PMN-0.08PT wafer, hence causes a big retarded phase value. It is significantly different to other SLMs[6~10].

4 Conclusions

A pair of time - varying 1D-BPMs is equivalent to a single time-varying 2D-BPM for speckle reduction in laser display system. To avoid vibratory motion of phase diffusers, EO material can be employed to generate a dynamic phase modulator actuated electrically. 1D-BPMs model is built up by using PMN-0.08PT and electrodes. The light phase shifts of the parallel (z direction) and perpendicular (x direction) polarization components are deduced mathematically. The light phase shift is simulated through EFA according to the electrical field distribution inside PMN-0.08PT wafer on the submicron order. The simulation result shows that two 0.3-μm-wide electrodes on PMN-0.08PT wafer perform relatively uniform phase shift with the space between electrodes of 3 μm.

References

1 J. W. Goodman. Some fundamental properties of speckle[J]. *J. Opt. Soc. Am.*, 1976, **66**(11): 1145~1150

2 J. I. Trisnadi. Hadamard speckle contrast reduction[J]. *Opt. Lett.*, 2004, **29**(1): 11~13

3 J. I. Trisnadi. Speckle contrast reduction in laser projection displays[C]. *SPIE*, 2002, **4657**: 131~137

4 J. I. Trisnadi, C. B. Carlisle, R. Monteverde. Overview and applications of grating light valve based optical write engines for high-speed digital imaging[C]. *SPIE*, 2004, **5348**: 52~64

5 Wenhong Gao, Zhaomin Tong, Vladimir Kartashov *et al*.. Replacing two dimensional binary phase matrix by a pair of one dimensional dynamic phase matrices for laser speckle reduction[J]. *J. Display Technol.*, 2012, **8**(5): 291~295

6 P. Shames, P.-C. Sun, Y. Fainman. Modeling and optimization of electro-optic phase modulator[C]. *SPIE*, 1996, **2693**: 787~796

7 P. E. Shames, P. C. Sun, Y. Fainman. Modeling of scattering and depolarizing electro-optic devices. I. Characterization of lanthanum-modified lead zirconate titanate[J]. *Appl. Opt.*, 1998, **37**(17): 3717~3725

8 P. E. Shames, P. C. Sun, Y. Fainman. Modeling of scattering and depolarizing electro-optic devices Ⅱ. Device simulation [J]. *Appl. Opt.*, 1998, **37**(17): 3726~3734

9 Q. W. Song. High efficiency electro-optic grating for optical switch[J]. *J. Mod. Opt.*, 1994, **41**(4): 717~727

10 Q. W. Song. High-efficiency electro-optical grating switch with improved performance[J]. *Appl. Opt.*, 1996, **35**(35): 7031~7036

11 A. Yariv, P. Yeh. Optical Waves in Crystals Propagation and Control of Laser Radiation[M]. New York: Wiley, 1984

12 M. Title, S.H. Lee. Modeling and characterization of embedded electrode performance in transverse electro optic modulators [J]. *Appl. Opt.*, 1990, **29**(1): 85~98

13 H. Jiang. Transparent electro-optic ceramics and devices[C]. *SPIE*, 2005, **5644**: 380~394